Assessing vaccine-mediated protection in an ultra-low dose *Mycobacterium tuberculosis* murine model

*Plumlee, C.R.[1], *Barrett, H.W.[1,2], Shao, D.E.[3], Lien, K.A.[1], Cross, L.M.[1], Cohen, S.B.[1], Edlefsen, P.T[3], Urdahl, K.B.[1,4,5,6,†]

[1] Center for Global Infectious Disease Research, Seattle Children's Research Institute, Seattle, WA, 98109, USA

[2] University of Washington, Dept. of Global Health, Seattle, WA, 98109, USA

[3] Vaccine and Infectious Disease Division, Fred Hutch Cancer Center, Seattle, WA, 98109, USA

[4] University of Washington, Dept. of Immunology, Seattle, WA, 98109, USA

[5] University of Washington, Dept. of Pediatrics, Seattle, WA, 98109, USA

[6] Lead Contact

[†]Correspondence: Kevin.Urdahl@seattlechildrens.org

*Equal contributions

ABSTRACT

Despite widespread immunization with Bacille-Calmette-Guerin (BCG), the only currently licensed tuberculosis (TB) vaccine, TB remains a leading cause of mortality globally. There are many TB vaccine candidates in the developmental pipeline, but the lack of a robust animal model to assess vaccine efficacy has hindered our ability to prioritize candidates for human clinical trials. Here we use a murine ultra-low dose (ULD) *Mycobacterium tuberculosis* (Mtb) challenge model to assess protection conferred by BCG vaccination. We show that BCG confers a reduction in lung bacterial burdens that is more durable than that observed after conventional dose challenge, curbs Mtb dissemination to the contralateral lung, and, in a small percentage of mice, prevents detectable infection. These findings are consistent with the ability of human BCG vaccination to mediate protection, particularly against disseminated disease, in specific human populations and clinical settings. Overall, our findings demonstrate that the ultra-low dose Mtb infection model can measure distinct parameters of immune protection that cannot be assessed in conventional dose murine infection models and could provide an improved platform for TB vaccine testing.

53

54 **INTRODUCTION**

55 New and effective tuberculosis (TB) vaccines are urgently needed. Although BCG vaccination
56 can provide protection in infants and older children in some clinical settings[1-4], it has proven to
57 be inadequate to combat the global pandemic. There are numerous TB vaccine candidates in
58 the developmental pipeline[5], but it will not be feasible to conduct human efficacy trials for most
59 of them. The standard for assessing vaccine efficacy is prevention of disease, which occurs in
60 only a small percentage of infected individuals, resulting in dauting sample sizes and costs
61 needed to complete human trials. Unfortunately, identifying promising vaccine candidates to
62 prioritize for human efficacy trials has been hindered by the lack of reliable animal models that
63 adequately predict human TB vaccine efficacy[6,7].

64

65 Historically, mice have been the most commonly used model for testing TB vaccine candidates
66 due to their ease of use, cost-effectiveness, and the relative conservation of the mammalian
67 immune system. However, limitations in the current mouse model, in which mice are infected
68 with ~50-100 CFU by aerosol, have shaken confidence regarding how well findings in mice can
69 be translated to humans[6,7]. There is minimal variability in the performance of different vaccines
70 in the current model. Most TB vaccines confer ~1 log of protection, reducing the lung burden
71 from ~10^6 to ~10^5 CFU, but only if assessed 4-6 weeks after aerosol challenge. This protection
72 is transient and usually dissipates by 3-4 months post-infection (p.i.)[8,9]. Furthermore, it is
73 unclear if the vaccine-induced mechanisms that enable mice to transiently reduce their bacterial
74 burdens in the setting of an ultimately unsuccessful immune response are relevant to the types
75 of immunity required for long lasting protection against the clinical manifestations of human TB.
76 Because mice in this model are unable to eradicate, or even durably control Mtb, some have
77 suggested that mice may lack the fundamental immune effector molecules needed for Mtb
78 control[10]. The failure of mouse vaccine testing to reliably predict results in human TB vaccine

79 trials have reinforced these concerns about the relevance of the mouse model for TB vaccine
80 testing[6,7].
81

82 Recently we developed a physiologic ultra-low dose (ULD) (i.e., 1-3 CFUs) Mtb mouse infection
83 model that more closely resembles several aspects of human Mtb infection[11]. Here we test the
84 ability of the ULD challenge model to assess immunity conferred by BCG vaccination, the
85 vaccine for which the most human efficacy data exists. In contrast to the conventional dose
86 model, we show that BCG-vaccinated mice challenged with 1-3 Mtb CFU exhibit a more durable
87 reduction in lung bacterial burdens. Vaccinated mice had an increased ability to contain
88 infection to a single lung and prevent Mtb dissemination to the contralateral lung. Finally,
89 vaccinated mice exhibited a significantly higher proportion of animals with no detectable
90 infection. Thus, the ULD model provides a promising platform for TB vaccine testing, as it
91 affords the opportunity to measure distinct parameters of vaccine-mediated immunity that
92 cannot be assessed in the current mouse model.
93

94 **RESULTS**

95 **BCG-mediated reduction of lung bacterial burdens is transient in the current mouse**
96 **model.**

97 The capacity of BCG to mediate protection in C57BL/6 (B6) mice infected with 50-100 Mtb CFU
98 has been assessed by many labs, but we sought to repeat this experiment in our own hands to
99 directly compare the conventional dose with the ULD model. We subcutaneously immunized B6
100 mice with 10^6 BCG-Pasteur 8 weeks prior to aerosol challenge with H37Rv Mtb and determined
101 the lung bacterial burdens at days 42 and 120 post-infection. As previously shown[8,9], BCG
102 immunization provided about one log of protection against lung bacterial burden at day 42, but
103 this protection was transient and dissipated at later timepoints; there was no significant

104 difference in bacterial burdens between unimmunized and BCG-immunized mice at day 120
105 post-infection (**Figure 1)**.
106
107 **Measuring vaccine-mediated immunity in the ULD Mtb model.**
108 Next, we assessed the efficacy of BCG in the ULD aerosol Mtb challenge model, a model in
109 which the aerosolized dose is reduced with a goal of infecting only ~60-80% of the mice in the
110 infection chamber[11]. As previously described using an ULD infection of a pool of bar-coded Mtb
111 strains, the number founding strains detected using bar-codes after ULD infection approximates
112 a Poisson distribution; most mice are infected with a single founding Mtb strain, whereas fewer
113 are infected with two or three founding strains[11]. **Figure 2** depicts a BCG immunization
114 experiment in which we assessed the bacterial burdens in the right and left lungs separately and
115 in the spleen 9 weeks after aerosol ULD challenge. Amongst those mice with detectable
116 infection (>0 CFU), we observed that, compared to unimmunized mice, BCG-immunized mice
117 had lower overall lung bacterial burdens (pooling right and left lungs) (**Figure 2A**), and lower
118 spleen bacterial burdens (**Figure 2B**). We also observed that 7/20 of the unimmunized mice and
119 10/20 of the BCG-immunized mice had no detectable infection in either lung (**Figure 2A**), a
120 difference that was not statistically significant in this single experiment (p=0.53). While the same
121 seven mice with undetectable lung bacterial burdens also had no detectable splenic bacterial
122 burdens, two mice that did have detectable lung infection in the BCG-immunized group failed to
123 show evidence of splenic bacterial burdens (12/20 BCG-immunized mice had no recoverable
124 Mtb from their spleen, compared to 10/20 from the lungs). <u>Thus, BCG immunization may</u>
125 <u>prevent Mtb dissemination to the spleen or promote splenic Mtb clearance.</u>
126
127 To further assess the capacity of BCG immunization to restrict Mtb dissemination, we also
128 assessed bacterial burdens separately in the right and left lungs. <u>In the ULD model, since</u>
129 <u>infection is usually established by a single founding Mtb strain, the lungs are often infected</u>

130 unilaterally; most commonly, the right lung is infected because the right lung and bronchus are
131 larger than the left [11]. Our previous ULD studies using bar-coded Mtb strains showed that
132 bilateral lung infection usually represents the dissemination of a single Mtb strain from the
133 infection-seeded lung to the contralateral lung. In the experiment shown in **Figure 2**, we
134 observed that 5/10 of the BCG-immunized mice exhibited unilateral lung infection compared to
135 only 1/13 of the infected unimmunized mice (p= 0.023; **Figure 2C and D**). Of the two BCG-
136 immunized mice with pulmonary Mtb infection but no detectable splenic bacterial burdens, one
137 was infected in the right lung only while the other had bilateral lung infection (**Figure 2D**). Thus,
138 the ULD model has the capacity to assess a vaccine's ability to prevent dissemination, a
139 parameter of protection that cannot be assessed in conventional dose infections because
140 dissemination occurs in all mice regardless of vaccination status.
141
142 **BCG confers durable reductions in lung bacterial burdens in ULD-challenged mice.**
143 As previously shown[8,9], and as demonstrated in **Figure 1**, BCG-mediated reductions in lung
144 bacterial burdens are abrogated by 100-120 days post-challenge. To assess the durability of
145 BCG-mediated protection in the ULD model, we performed a time course and assessed
146 bacterial burdens in the lungs and spleen of ULD-infected mice at an early (d14), intermediate
147 (d42), and late timepoint (d115). Because ULD challenge results in some mice with no
148 detectable lung bacteria, even in the absence of immunization, we assessed bacterial burdens
149 only in mice with detectable bacterial burdens and performed a separate analysis to determine
150 the proportion of mice with undetectable bacteria (the latter is shown in **Figure 5**). At day 14
151 post ULD-infection, bacterial burdens were similar in both unimmunized and BCG-immunized
152 infected mice, but at days 42 and 115, bacterial burdens were reduced by approximately one
153 log (p=0.002 and p<0.001, respectively, excluding those with 0 CFU; **Figure 3A**). These data
154 suggest that BCG-mediated reductions of lung bacterial burdens are more durable in ULD-

155 infected mice compared to conventional dose-infected mice, but the intentional heterogeneous
156 nature of the model makes it difficult to draw conclusions based on a single experiment.
157
158 Next, we performed multiple ULD challenge experiments comparing BCG immunized vs.
159 unimmunized mice to rigorously assess the reproducibility of our findings. **Supplemental Table**
160 **1** shows results from 31 individual experiments assessing BCG efficacy in the ULD model,
161 representing a total of 537 unimmunized and 543 BCG-immunized mice with lung bacterial
162 burdens assessed at timepoints ranging from days 14-125 post-infection. **Figure 3B** shows the
163 combined (right and left lungs pooled) bacterial burdens from all experiments binned by similar
164 timepoints post-infection. Similar to prior reports using a conventional dose Mtb challenge[12,13],
165 BCG had no effect on bacterial burdens at the earliest timepoints assessed, days 14-15 post-
166 infection. However, BCG-immunized mice had lower lung bacterial burdens than unimmunized
167 mice at every later timepoint (excluding those with 0 CFU). This reduction remained robust (~1
168 log) even at days 90-125 post-infection. Thus, unlike the transient reduction of bacterial burdens
169 observed in the conventional dose Mtb challenge model[8,9], BCG durably reduces the lung
170 bacterial burdens in ULD-challenged mice for at least 4 months post-infection.
171
172 **BCG prevents Mtb dissemination to the contralateral lung.**
173 To better assess the reproducibility of BCG's capacity to prevent dissemination, we assessed
174 the proportion of mice with bilateral vs. unilateral lung infection in all experiments shown in
175 **Supplemental Table I**. Based on raw CFU data, there was no difference in the proportion of
176 mice with bilateral lung infection between unimmunized vs. BCG-immunized groups at days 14-
177 15 post-infection. At this early timepoint, the proportion of mice with bilateral lung infection was
178 low even in unimmunized mice, suggesting that dissemination had not yet occurred in either
179 group. This conclusion is supported by the observation that <20% of ULD-infected mice had
180 detectable splenic Mtb burdens at d14 post-infection (data not shown). At all later timepoints,

181 however, the proportion of mice with bilateral lung infection was higher in unimmunized
182 compared to BCG-immunized mice even out to days 90-125 post-infection (**Figure 4A**).
183 Although bilateral lung infection in the ULD model usually reflects Mtb dissemination from the
184 initially infected lung to the contralateral lung, it can sometimes represent separate aerosolized
185 infections by distinct bacilli in each individual lung. To assess true dissemination more
186 accurately, we ULD-infected mice with a pool of 50 bar-coded H37Rv Mtb strains that we have
187 previously characterized[11]. Amplified genomic DNA extracted from bacterial colonies of each
188 infected mouse lung were sequenced to determine the number of unique founding Mtb strains in
189 each lung (**Figure 4B**). Because the probability of separate infections with the same bar-coded
190 strain is only ~1 in 78 when using the 50 bar-coded Mtb pool in the ULD model[11], bilateral lung
191 infection with a single Mtb strain in both lungs likely represents true dissemination (e.g. BCG
192 36L and 36R). In contrast, when mice have different Mtb strains in each lung (e.g. BCG 28L and
193 28R), this reflects separate infections of each lung. Thus, if dissemination to the contralateral
194 lung is assessed by bacterial burden alone without assessing Mtb bar-codes, the ability of a
195 vaccine to prevent dissemination will be underestimated due to falsely categorizing separate
196 infections in each lung as dissemination events. In this experiment, BCG was deemed to have
197 50.2% efficacy ($p = 0.002$); **Figure 4C**) in preventing dissemination when measured as the
198 proportion of mice with bilateral Mtb infection. However, if dissemination was defined as the
199 proportion of mice that possessed at least one identical bar-coded Mtb strain in both lungs, then
200 BCG exhibited an efficacy of 73.5% ($p = 0.001$, **Figure 4D**). Compiling data from all
201 experiments in which we performed bar-coded infection and sequencing (n=5) revealed that
202 BCG exhibited 79.7% efficacy in preventing dissemination of Mtb to the contralateral lung ($p <$
203 0.001; **Figure 4E**).
204
205 **BCG immunization can prevent detectable infection.**

206 Finally, we compared the proportion of unimmunized and BCG-immunized mice that presented
207 with undetectable pulmonary infection. Pooling the data from all experiments assessed at D14-
208 15 after Mtb challenge (n=6), we observed no difference in the proportion of mice with
209 undetectable bacterial burdens in the BCG-immunized vs. unimmunized groups (**Figure 5A**).
210 However, at all later timepoints through day 125 post-infection, we observed more mice with
211 undetectable bacterial burdens in BCG-immunized mice than in unimmunized mice. Excluding
212 the six experiments assessed at D14-15 when no difference was seen, we plotted the remaining
213 25 experiments at timepoints from D26-125 as the proportion of mice with undetectable
214 bacterial burdens in the unimmunized vs. BCG-immunized group (**Figure 5B**). Although only
215 three experiments (15-20 mice/group/experiment) reached statistical significance on their own
216 (all in the BCG-immunized group), most experiments (18 of 25) had a higher proportion of mice
217 with undetectable bacterial burdens in the BCG-immunized group. When the compiled data from
218 all 25 of these experiments were assessed (**Figure 5B**, black filled circle), the difference in the
219 proportion of mice with undetectable bacterial burdens in the BCG-immunized compared to the
220 unimmunized group was relatively modest (13% efficacy in preventing detectable infection), but
221 highly statistically significant ($p = 0.001$).
222
223 We also examined the number of founding strains in each mouse for all ULD experiments using
224 the pool of bar-coded strains (9 experiments with unimmunized mice and 6 with BCG-
225 immunized) (**Figure 5C**). As expected from the Poisson distribution, most unimmunized mice
226 were infected with only one strain, and fewer mice were infected with two or more strains. There
227 were similar proportions of unimmunized and BCG-immunized mice infected with two or more
228 Mtb strains. However, fewer BCG-immunized mice were infected with one founding Mtb strain
229 (36.9% of unimmunized mice versus 22.9% of BCG-immunized mice, $p = 0.011$), whereas more
230 BCG-immunized mice had zero Mtb strains (33.0% of unimmunized mice versus 48.3% of BCG-
231 immunized mice, $p = 0.008$). This suggests that infection attributable to a single founding Mtb

232 strain may be more readily prevented by BCG-mediated immunity than infection due to two or
233 more strains, but further investigation is needed to test this possibility more rigorously.
234
235 The demonstration that vaccine-induced immunity can prevent detectable Mtb infection in ULD-
236 infected mice opens the possibility of assessing a new and important immune parameter for TB
237 vaccine testing that was not known to be achievable in mice. However, BCG had a very low
238 capacity to mediate this type of protection (13% efficacy, $p = 0.001$); large numbers of mice
239 were required to reach statistical significance, which would not be practical for routine testing of
240 TB vaccine candidates. Because the overarching goal is to identify vaccines that are more
241 efficacious than BCG, we performed a power calculation to determine what level of vaccine
242 efficacy would be required to feasibly measure prevention of infection with a reasonable number
243 of mice (**Table 1)**. This analysis showed that a vaccine with 50-60% efficacy could be assessed
244 with a sample size of 28-55 mice per group, which would be achievable by pooling results from
245 2-3 experiments. Such a pipeline could be feasible, as Vidal et al. recently reported that a novel
246 live attenuated Mtb vaccine was dramatically more effective than BCG in the ULD challenge
247 model, and prevention of detectable infection could be measured in a statistically significant
248 manner with only 18 mice per group[25]. Taken together with our findings, these results suggest
249 that the ULD challenge model provides a larger window to measure differences between TB
250 vaccine candidates and to measure parameters of protection, including inhibition of
251 dissemination and prevention of detectable infection, that cannot be assessed in currently used
252 mouse models.
253
254 **DISCUSSION**
255 Despite widespread vaccination with BCG, TB remains a major cause of global morbidity and
256 mortality[14]. Although surpassed for a couple years by SARS-CoV-2 as the leading cause of
257 death due to a single infectious organism, recent mortality estimates for each infection suggest

258 that TB is again the number one cause of infectious death[14]. New vaccines that provide better
259 efficacy than BCG are needed. To triage the growing number of TB vaccine candidates and
260 move those with the most promise into clinical trials, there is an urgent need to develop small
261 animal models that reliably assess parameters of immunity with relevance to human protection.
262 There is growing concern that the current mouse model, in which mice are infected with 50-100
263 Mtb CFU by aerosolization, is not up to this task[6,7]. This model provides too small a window to
264 discern differences between vaccine candidates; most confer a transient reduction in the lung
265 bacterial burden by about one log if measured between 4-6 weeks post-infection. Durable
266 reductions in lung bacterial burdens and other clinically relevant parameters of immunity,
267 including the ability to curb Mtb dissemination or prevent detectable infection, are difficult or
268 impossible to assess. Indeed, the inability of the current model to predict how well vaccine
269 candidates will perform in human efficacy trials is becoming increasingly apparent[6,7]. In this
270 study, we demonstrate that the ULD murine model provides a promising new challenge model in
271 which three distinct parameters of protection can be assessed: 1) reductions in lung bacterial
272 burdens <u>that are more durable than after conventional dose challenge</u>, 2) inhibition of Mtb
273 dissemination, and 3) prevention of detectable infection.
274
275 Of these, reduction in bacterial burdens is the only parameter of protection that can readily be
276 assessed in current mouse models. In contrast to transient protection that dissipates within 3-4
277 months in the current model[8,9], we have shown durable lung bacterial burden reductions for at
278 least four months in the ULD model. Importantly, the types of immune responses that mediate
279 reductions in lung bacterial burdens in mice infected with high doses (>250 CFUs) are
280 sometimes different than those that do so at conventional doses (50–100 CFU)[15,16]. Although
281 this has not yet been rigorously assessed in the ULD model, it is reasonable to hypothesize that
282 the optimal immune responses that are optimal for reducing lung bacterial burdens after a
283 physiologic dose challenge of 1-3 CFU may also be different than those required for a 50-100

284 CFU challenge. Thus, vaccine candidates may vary in their capacity to control bacterial burdens
285 to a physiologically relevant challenge dose compared to a challenge dose that is artificially
286 high, a hypothesis that needs further investigation.
287
288 The second parameter of immunity that can be measured in the ULD model is the ability to
289 prevent dissemination. Because most ULD-infected mice are infected by a single founding
290 bacillus[11], infection is usually initiated at a single site in one lung. Thus, most bilateral lung
291 infection is the result of Mtb dissemination from the initially infected lung to the contralateral lung
292 and CFU determinations of each individual lung can provide an estimation of a vaccine's ability
293 to block dissemination, which we have termed containment. This approach underestimates
294 containment, however, because some mice may have Mtb in each lung not because of
295 dissemination, but due to independent infection events of each lung by two or more distinct
296 aerosolized strains. By infecting mice with a pool of bar-coded strains, we have shown that we
297 can distinguish between disseminated infection and separate infections with different strains by
298 sequencing the Mtb bar-codes in each lung. Using this approach, we have shown that BCG
299 immunization can prevent Mtb dissemination to the contralateral lung in ~80% of ULD-infected
300 mice. These results in the murine ULD model parallel results in BCG vaccinated humans
301 showing that BCG vaccination is most effective at preventing disseminated forms of TB[17].
302
303 The third parameter of immunity that can be assessed in the ULD model is the prevention of
304 detectable infection. There are several lines of evidence that the human immune system can
305 prevent or eradicate Mtb infection. Some individuals with high exposure to index cases with
306 active TB disease, including household contacts, fail to develop an Mtb-specific IFNγ-producing
307 T cell response, suggesting that long-term Mtb infection is sometimes not established despite
308 intense exposure[18]. Furthermore, many individuals that do develop a T cell IFNγ response

309 against Mtb may eventually eradicate infection, as the incidence of active TB is quite low
310 amongst IGRA+ individuals (usually less than 5%) even when their immune systems are
311 potently immunosuppressed or ablated[19]. Recently there have been several high-profile TB
312 vaccine studies showing that some vaccines can prevent detectable infection in non-human
313 primates[20-22]. This had not been previously shown in mice, and it has been postulated that mice
314 lack the fundamental immune effectors needed to prevent sustained Mtb infection[10]. In this
315 study we showed no difference in the proportion of BCG-immunized mice with detectable
316 infection compared to controls at d14-15 after Mtb challenge, suggesting that vaccination did not
317 block the initial Mtb infection. At all later timepoints, however, BCG vaccinated animals had a
318 modest, but highly statistically significant increase in the proportion of mice with undetectable
319 infection compared to unimmunized controls (overall 13% efficacy, p=0.001). This suggests that
320 a small proportion of the vaccinated mice that may have been initially infected were able to clear
321 Mtb to undetectable levels. Even though BCG can do this only modestly, these results suggest
322 that vaccine-mediated immunity can prevent sustained infection in mice exposed to a
323 physiologic Mtb dose, challenging the longstanding belief stemming from experiments with an
324 artificially high Mtb exposure dose, that mice are unable to eradicate Mtb infection.
325
326 One limitation of the ULD model for vaccine testing is the number of animals that are required in
327 each group. This is exacerbated by the fact that not all animals are initially infected in the model,
328 and currently it is not possible to discern animals that were never infected from those that were
329 initially infected, but subsequently eradicated Mtb. We have attempted to develop both
330 immunologic and molecular assays to distinguish between these possible outcomes, but this
331 has proven difficult to achieve. We initially assessed Mtb-specific CD4 T cell responses against
332 an Mtb antigen (ESAT-6) that is not present in BCG. We identified a couple unvaccinated mice
333 that were exposed to aerosolized ULD Mtb and had measurable Mtb ESAT-6-specific CD4 T
334 cell responses despite having no detectable lung bacterial burdens. These results suggested

335 that even a few unvaccinated ULD-infected mice may clear Mtb to undetectable levels, but mice
336 exhibiting this phenotype were rare. However, this approach was not successful in BCG-
337 immunized mice because BCG immunization suppressed the development of Mtb ESAT-6-
338 specific T cells to undetectable or almost undetectable levels even in ULD Mtb-challenged mice
339 that were demonstrably infected, providing minimal window to discern differences between
340 uninfected and infected mice. We also attempted to amplify Mtb DNA from lung homogenate
341 using previously published Mtb-specific PCR primers[23]. Unfortunately, the sensitivity of this
342 assay was not sufficient to reliably detect below 1,000 viable bacteria, and we were unable to
343 obtain a signal from mice with undetectable bacterial burdens. Despite our inability to
344 differentiate mice that were never infected from those who cleared infection, we were able to
345 build strong statistical evidence for prevention of detectable infection by assessing large
346 numbers of mice.
347
348 Our results are consistent with findings that BCG can sometimes provide long-term protection
349 against human TB, and are consistent with studies showing BCG-mediated protection in
350 individuals without prior Mtb exposure (tuberculin skin test-negative or IGRA-negative
351 individuals) or in low Mtb transmission settings[1-4]. The low overall observed efficacy (~13%) in
352 preventing detectable infection also reflects the suboptimal nature of BCG-mediated immunity.
353 Reliably assessing this parameter of protection for a vaccine with such low efficacy would
354 require hundreds of mice per group, as in this study, which would not be feasible for routine pre-
355 clinical evaluation of TB vaccine candidates. However, the goal is to identify promising vaccine
356 candidates that are significantly more efficacious than BCG to move into human trials. Our
357 power analysis showed that a vaccine with 50% efficacy could be readily assessed by repeating
358 studies with 15-20 mice per group 2-3 times and compiling the results. We believe this is
359 feasible and would be worthwhile if further studies show that results obtained in the ULD model
360 are superior to those obtained in the conventional murine model for distinguishing vaccine

361 efficacies in clinical meaningful ways. We are encouraged that a recent study assessing a novel
362 TB vaccine candidate (ΔLprG, a live-attenuated Mtb vaccine) in the ULD mouse model showed
363 that ΔLprG was dramatically better than BCG at preventing detectable infection and achieved
364 statistical significance with only 18 mice per group[25]. In this same study, ΔLprG was only slightly
365 better than BCG in reducing lung bacterial burdens in mice challenged with 100 CFU,
366 suggesting that the ULD challenge model provides a larger window to discriminate differences
367 between vaccines.
368
369 Overall, the ULD challenge model holds promise as a new and improved platform for evaluating
370 TB vaccine candidates. The model can assess distinct parameters of vaccine-mediated
371 immunity that cannot be assessed in the current mouse model and has potential to improve
372 discrimination between the protective capacities of different vaccines. Each of the three
373 parameters of immunity that can be assessed in the ULD model may be relevant to different
374 clinical TB outcomes. For example, the ability of vaccines to durably reduce lung bacterial
375 burdens and prevent dissemination may reflect their capacity to prevent different aspects of TB
376 disease, whereas the ability to prevent detectable infection may reflect prevention of sustained
377 infection. Because each of these parameters are likely mediated by different aspects of
378 immunity, it is possible that different vaccines will differ in the relative capacity to control Mtb
379 burdens, inhibit dissemination, and prevent detectable infection. Future studies are needed to
380 assess a variety of TB vaccine candidates in the ULD model, and whenever possible, determine
381 whether the results correlate with clinical outcomes in human vaccine trials.
382
383 **ACKNOWLEDGMENTS**
384 The authors would like to thank Bridget Alexander, Lindsay Engels, Samuel Schrader, Kaitlin
385 Durga and the Seattle Children's OAC staff for technical support. This work was supported by

NIH contract 75N93019C00070 (K.B.U), the Bill and Melinda Gates Foundation, INV-026296 (K.B.U) and NIH grant U19AI135976 (K.B.U).

FIGURE LEGENDS

Figure 1. BCG-mediated reductions in Mtb lung burdens are not durable in a conventional-dose infection. C57BL/6 (B6) mice were aerosol infected with a conventional dose (CD) (50-100 CFU) of H37Rv Mtb eight weeks following either subcutaneous (s.c.) immunization with 10^6 BCG-Pasteur (BCG) or no immunization (unimmunized). On day 42 or 120 post-infection, CFU were enumerated from lung homogenates plated onto 7H10 plates. These data represent 5 mice per group and are shown as mean ± SEM. Single-group comparisons were analyzed using an unpaired t test. ***p<0.001.

Figure 2. Assessing BCG efficacy in the ultra-low dose Mtb model. B6 mice were aerosol infected with an ULD (1-3 CFU) of H37Rv Mtb 8 weeks following either s.c. immunization with 10^6 BCG-Pasteur (n=20) or no immunization (n=20). On day 63 post-infection, CFU were enumerated from left lung, right lung, or spleen homogenates plated onto 7H10 plates. **A)** Combined lung CFUs or **B)** spleen CFUs from unimmunized and BCG-immunized mice are graphed. Counts from left lungs, right lungs and spleen are graphed separately from, **C)** unimmunized mice or **D)** BCG-immunized mice. There were 20 mice per group, and the data are graphed as mean ± SD. Single-group comparisons were analyzed using an unpaired t test <u>and excluding mice with 0 CFU</u>. **p<0.01, ****p<0.0001.

Figure 3. BCG-mediated reductions in Mtb lung burden are <u>more</u> durable in the ULD model. A) Combined lung CFU from a single experiment time course of ULD-infected B6 mice with or without BCG immunization. Combined lung CFU were enumerated on days 14, 42, and 115 post-infection. There were 19 or 20 mice per group, and the data are graphed as mean ±

412 SD. Single-group comparisons were analyzed using an unpaired t test (excluding mice with 0
413 CFU). ***p<0.001, ****p<0.0001. **B)** Combined lung CFU from a compilation of 31 experiments,
414 excluding mice with 0 CFU, separated by timepoint post-infection of ULD-infected B6 mice with
415 or without BCG immunization. Error bars are 95% confidence intervals in a fixed effects
416 negative regression model. All timepoints except days 14-15 post-infection have a $p < 0.001$.
417
418 **Figure 4. BCG-immunization prevents Mtb dissemination to the contralateral lung. A)**
419 Proportion of mice with bilateral lung infection (CFU in left and right lung) from a compilation of
420 31 experiments separated by timepoint post-infection of ULD-infected B6 mice with or without
421 BCG immunization. Error bars are 95% confidence intervals in a mixed effects logistic
422 regression model, with experiment as a grouping variable. All timepoints except days 14-15
423 post-infection have a $p \leq 0.001$. **B)** A single ULD experiment using bar-coded Mtb strains is
424 shown. On day 65 post-infection, right and left lung homogenates were plated onto 7H10 plates
425 and Mtb colonies from infected lungs were scraped to make genomic DNA. DNA was
426 sequenced, and the identity of each bar-coded Mtb strain is graphed for each lung separately.
427 The percentage of bilateral infection for unimmunized and BCG-immunized mice from this
428 experiment was calculated by the proportion of mice with CFUs in both lungs **(C)** or the
429 proportion of mice with at least one common Mtb strain in both lungs **(D)**. **(E)** The percentage of
430 mice with bilateral Mtb strains was compiled from 5 independent experiments, excluding day 14
431 post-infection. Vaccine efficacy for preventing dissemination to the contralateral lung was
432 calculated as 1-(% BCG mice with bilateral infection)/(% Unimmunized mice with bilateral
433 infection).
434
435 **Figure 5. BCG immunization prevents detectable infection in some mice. A)** Table of all
436 mice, showing the percentage with 0 CFU in the unimmunized vs BCG-immunized groups
437 separated by timepoint post-infection. **B)** The proportion of unimmunized mice with 0 CFU (x-

438 axis) vs the proportion of BCG-immunized mice with 0 CFU (y-axis) for each experiment from a
439 compilation of 25 experiments (days 26-125) separated by timepoint post-ULD infection. Each
440 colored symbol is an independent experiment, and the larger black circle is the compilation of all
441 the data, which was statistically significant (mixed effects logistic regression $p = 0.001$). Post-
442 hoc analyses indicated that, if each infection cohort had been analyzed separately, the 3 filled in
443 symbols would have attained statistical significance if they had been analyzed using the same
444 regression model ($p<0.05$), see supplemental Figure 1. **C)** In ULD-Mtb experiments in which
445 bar-coded strains were used for infection (n=9 for unimmunized, n=6 for BCG-immunized), the
446 mice are graphed according to the number of unique Mtb strains recovered from each mouse's
447 lungs.
448
449 **Table 1. Group sizes needed to assess vaccine-mediated prevention of detectable**
450 **infection.** Minimum sample size required per group for specified power to detect a given
451 vaccine efficacy (prevalence in unimmunized mice assumed to be 61.6%).
452
453 **METHODS**
454 **Mice**
455 C57BL/6J mice were purchased from Jackson Laboratories (Bar Harbor, ME). Female mice
456 between the ages of 9-12 weeks were used. All animals were housed and maintained in
457 specific-pathogen-free conditions at Seattle Children's Research Institute (SCRI). All animal
458 studies were performed in compliance with the SCRI Animal Care and Use Committee.
459
460 **BCG Immunizations**
461 BCG-Pasteur was cultured in Middlebrook 7H9 with OADC supplement and 0.05% Tween-80 at
462 37˚C with constant agitation for five days. BCG was back diluted in 7H9 for two days and grown

463 to an OD of 0.2-0.5. Bacteria was diluted in PBS and mice were injected subcutaneously with
464 200µl of 10^6 CFU. After immunization, mice were rested for 8 weeks prior to Mtb infection.
465
466 **ULD Mtb Aerosol Infections**
467 H37Rv or bar-coded H37Rv Mtb were used for infections[11]. Mtb stocks were grown in
468 Middlebrook 7H9 with OADC supplement and 0.05% Tween-80 at 37˚C with constant agitation
469 to an OD = 1. Cultures were filtered through a 5µm filter to remove clumps and aliquots were
470 frozen at -80˚C. Frozen filtered stocks were thawed and titered side by side with stocks used for
471 conventional dose infection to determine how to dilute the ULD stocks with the goal of leaving
472 37% of mice uninfected. Mice were infected using a Glas-Col aerosol infection chamber.
473
474 **CFU Plating**
475 Mouse organs (right lung, left lung, or spleen) were homogenized separately in M tubes
476 containing 1mL PBS+0.05% Tween-80 (PBS-T) using a Miltenyi GentleMACS machine
477 (Miltenyi). Homogenates were then diluted in PBS-T and plated onto 7H10 plates. For ULD
478 infections, undiluted homogenate was also plated between two 7H10 plates. Plates were
479 incubated at 37˚C for at least 21 days before quantification of CFU.
480
481 **Genomic DNA Extraction**
482 Bacterial colonies grown from infected left lungs or right lungs were scraped into resuspension
483 buffer (25mM Tris-HCl pH 7.9, 10mM EDTA, 50mM glucose, water) plus 10mg/mL lysozyme
484 and were incubated at 37˚C overnight. Samples were resuspended in 10% sodium dodecyl
485 sulfate and 10mg/mL Proteinase K and were heated at 55˚C for 30 minutes. Samples were then
486 resuspended in 5M NaCl followed by Cetrimide saline solution and heated at 65˚C for 10
487 minutes. Genomic DNA was extracted twice with 24:1 chloroform:isoamyl alcohol. DNA was

488 precipitated with 0.7x volume of isopropanol and washed with 70% ethanol. Finally, DNA was
489 eluted with DEPC water.
490
491 **Barcoded Sequencing**
492 Mice were infected with a pool of 50 bar-coded strains. Sequencing of bacterial bar-codes has
493 been previously described[11,24]. Briefly, genomic DNA was pre-amplified with pooled barcoded
494 primers before libraries were prepared with NEBNext Ultra DNA Library Prep Kit for Illumina
495 (New England Biolabs) using the AMPure XP reagent (AgenCourt Bioscience) for size selection
496 and cleanup. The NEBNext Multiplex Oligos for Illumina (New England Biosciences) were used
497 to barcode DNA libraries and enabled multiplexing of 96 libraries per sequencing run. Samples
498 were sequenced using the NextSeq 500 Mid Output v2 kit (Illumina) at the University of
499 Washington Northwest Genomics Center. Read alignment was carried out using a custom
500 processing pipeline that has been previously described[24].
501
502 **Statistics**
503 All statistical analysis was done in R v.4.2.0 with packages Exact (v3.1) and lme4 (v1.1-30).
504 When comparing values between two groups in a single experiment, we used Barnard's exact
505 test for differences in proportions and simple linear regression on log-transformed CFU values
506 for differences in bacterial burden (excluding those with 0 CFU). For analyses compiling more
507 than one experiment, we used mixed effects logistic regression with experiment as the grouping
508 variable for differences in proportions, and mixed effects linear regression on log-transformed
509 CFU values for differences in bacterial burden. In all analyses, mice were considered protected
510 when the CFU was undetectable in both lungs, and analyses of dissemination and overall
511 bacterial burden were performed conditional on absence of protection.
512
513 **REFERENCES**

1. Colditz, G.A., Berkey, C.S., Mosteller, F., Brewer, T.F., Wilson, M.E., Burdick, E., and Fineberg, H.V. (1995). The efficacy of bacillus Calmette-Guerin vaccination of newborns and infants in the prevention of tuberculosis: meta-analyses of the published literature. Pediatrics *96*, 29-35.
2. Mangtani, P., Abubakar, I., Ariti, C., Beynon, R., Pimpin, L., Fine, P.E., Rodrigues, L.C., Smith, P.G., Lipman, M., Whiting, P.F., and Sterne, J.A. (2014). Protection by BCG vaccine against tuberculosis: a systematic review of randomized controlled trials. Clin Infect Dis *58*, 470-480. 10.1093/cid/cit790.
3. Abubakar, I., Pimpin, L., Ariti, C., Beynon, R., Mangtani, P., Sterne, J.A., Fine, P.E., Smith, P.G., Lipman, M., Elliman, D., et al. (2013). Systematic review and meta-analysis of the current evidence on the duration of protection by bacillus Calmette-Guerin vaccination against tuberculosis. Health Technol Assess *17*, 1-372, v-vi. 10.3310/hta17370.
4. Trauer, J.M., Kawai, A., Coussens, A.K., Datta, M., Williams, B.M., McBryde, E.S., and Ragonnet, R. (2021). Timing of Mycobacterium tuberculosis exposure explains variation in BCG effectiveness: a systematic review and meta-analysis. Thorax *76*, 1131-1141. 10.1136/thoraxjnl-2020-216794.
5. Schrager, L.K., Vekemens, J., Drager, N., Lewinsohn, D.M., and Olesen, O.F. (2020). The status of tuberculosis vaccine development. Lancet Infect Dis *20*, e28-e37. 10.1016/S1473-3099(19)30625-5.
6. Karp, C.L., Wilson, C.B., and Stuart, L.M. (2015). Tuberculosis vaccines: barriers and prospects on the quest for a transformative tool. Immunol Rev *264*, 363-381. 10.1111/imr.12270.
7. Cardona, P.J., and Williams, A. (2017). Experimental animal modelling for TB vaccine development. Int J Infect Dis *56*, 268-273. 10.1016/j.ijid.2017.01.030.
8. Lindenstrom, T., Knudsen, N.P., Agger, E.M., and Andersen, P. (2013). Control of chronic mycobacterium tuberculosis infection by CD4 KLRG1- IL-2-secreting central memory cells. J Immunol *190*, 6311-6319. 10.4049/jimmunol.1300248.
9. Nemeth, J., Olson, G.S., Rothchild, A.C., Jahn, A.N., Mai, D., Duffy, F.J., Delahaye, J.L., Srivatsan, S., Plumlee, C.R., Urdahl, K.B., et al. (2020). Contained Mycobacterium tuberculosis infection induces concomitant and heterologous protection. PLoS Pathog *16*, e1008655. 10.1371/journal.ppat.1008655.
10. Bloom, B.R., and Modlin, R.L. (2016). Mechanisms of Defense against Intracellular Pathogens Mediated by Human Macrophages. Microbiol Spectr *4*. 10.1128/microbiolspec.MCHD-0006-2015.
11. Plumlee, C.R., Duffy, F.J., Gern, B.H., Delahaye, J.L., Cohen, S.B., Stoltzfus, C.R., Rustad, T.R., Hansen, S.G., Axthelm, M.K., Picker, L.J., et al. (2021). Ultra-low Dose Aerosol Infection of Mice with Mycobacterium tuberculosis More Closely Models Human Tuberculosis. Cell Host Microbe *29*, 68-82 e65. 10.1016/j.chom.2020.10.003.
12. Mollenkopf, H.J., Kursar, M., and Kaufmann, S.H. (2004). Immune response to postprimary tuberculosis in mice: Mycobacterium tuberculosis and Miycobacterium bovis bacille Calmette-Guerin induce equal protection. J Infect Dis *190*, 588-597. 10.1086/422394.
13. Delahaye, J.L., Gern, B.H., Cohen, S.B., Plumlee, C.R., Shafiani, S., Gerner, M.Y., and Urdahl, K.B. (2019). Cutting Edge: Bacillus Calmette-Guerin-Induced T Cells Shape

560 Mycobacterium tuberculosis Infection before Reducing the Bacterial Burden. J Immunol
561 *203*, 807-812. 10.4049/jimmunol.1900108.
562 14. Bagcchi, S. (2023). WHO's Global Tuberculosis Report 2022. Lancet Microbe *4*, e20.
563 10.1016/S2666-5247(22)00359-7.
564 15. Maglione, P.J., Xu, J., and Chan, J. (2007). B cells moderate inflammatory progression
565 and enhance bacterial containment upon pulmonary challenge with Mycobacterium
566 tuberculosis. J Immunol *178*, 7222-7234. 10.4049/jimmunol.178.11.7222.
567 16. Mayer-Barber, K.D., Andrade, B.B., Barber, D.L., Hieny, S., Feng, C.G., Caspar, P.,
568 Oland, S., Gordon, S., and Sher, A. (2011). Innate and adaptive interferons suppress IL-
569 1alpha and IL-1beta production by distinct pulmonary myeloid subsets during
570 Mycobacterium tuberculosis infection. Immunity *35*, 1023-1034.
571 10.1016/j.immuni.2011.12.002.
572 17. Fine, P.E. (1988). BCG vaccination against tuberculosis and leprosy. Br Med Bull *44*,
573 691-703. 10.1093/oxfordjournals.bmb.a072277.
574 18. Lu, L.L., Smith, M.T., Yu, K.K.Q., Luedemann, C., Suscovich, T.J., Grace, P.S., Cain,
575 A., Yu, W.H., McKitrick, T.R., Lauffenburger, D., et al. (2019). IFN-gamma-
576 independent immune markers of Mycobacterium tuberculosis exposure. Nat Med *25*,
577 977-987. 10.1038/s41591-019-0441-3.
578 19. Behr, M.A., Edelstein, P.H., and Ramakrishnan, L. (2019). Is Mycobacterium
579 tuberculosis infection life long? BMJ *367*, l5770. 10.1136/bmj.l5770.
580 20. Hansen, S.G., Zak, D.E., Xu, G., Ford, J.C., Marshall, E.E., Malouli, D., Gilbride, R.M.,
581 Hughes, C.M., Ventura, A.B., Ainslie, E., et al. (2018). Prevention of tuberculosis in
582 rhesus macaques by a cytomegalovirus-based vaccine. Nat Med *24*, 130-143.
583 10.1038/nm.4473.
584 21. Dijkman, K., Sombroek, C.C., Vervenne, R.A.W., Hofman, S.O., Boot, C., Remarque,
585 E.J., Kocken, C.H.M., Ottenhoff, T.H.M., Kondova, I., Khayum, M.A., et al. (2019).
586 Prevention of tuberculosis infection and disease by local BCG in repeatedly exposed
587 rhesus macaques. Nat Med *25*, 255-262. 10.1038/s41591-018-0319-9.
588 22. Darrah, P.A., Zeppa, J.J., Maiello, P., Hackney, J.A., Wadsworth, M.H., 2nd, Hughes,
589 T.K., Pokkali, S., Swanson, P.A., 2nd, Grant, N.L., Rodgers, M.A., et al. (2020).
590 Prevention of tuberculosis in macaques after intravenous BCG immunization. Nature
591 *577*, 95-102. 10.1038/s41586-019-1817-8.
592 23. Martin, C.J., Cadena, A.M., Leung, V.W., Lin, P.L., Maiello, P., Hicks, N., Chase, M.R.,
593 Flynn, J.L., and Fortune, S.M. (2017). Digitally Barcoding Mycobacterium tuberculosis
594 Reveals In Vivo Infection Dynamics in the Macaque Model of Tuberculosis. mBio *8*.
595 10.1128/mBio.00312-17.
596 24. Ma, S.M., R.; Hobbs, S.J.; Farrow-Johnson, J.; Rustad, T.R.; Sherman, D.R. (2018).
597 Network stress test reveals novel drug potentiators in Mycobacterium tuberculosis.
598 submitted.
599 25. Vidal, S.J., Sellers, D., Yu, J., Wakabayashi, S., Sixsmith, J., Aid, M., Barrett, J.,
600 Stevens, S.F., Liu, X., Li, W., Plumlee, C.R., Urdahl, K.B., Martinot, A.J., Barouch, D.H.
601 (2023). Attenuated Mycobacterium tuberculosis Vaccine Protection in a Low Dose
602 Murine Challenge Model. iScience 26:6. 10.1016/j.isci.2023.106963

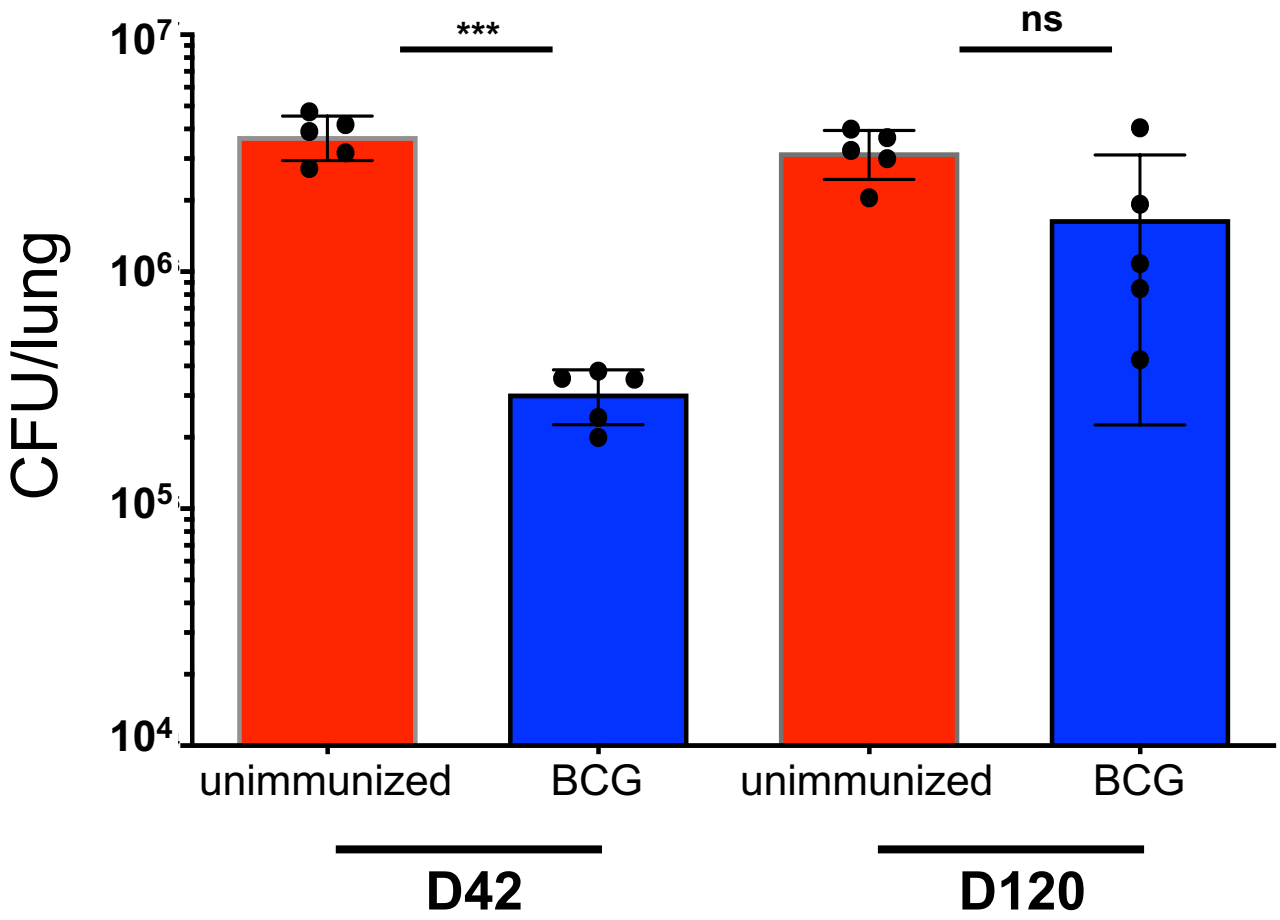
***
ns
10^7
10^6
10^5
10^4
CFU/lung
unimmunized
BCG
unimmunized
BCG
D42
D120

Figure 1

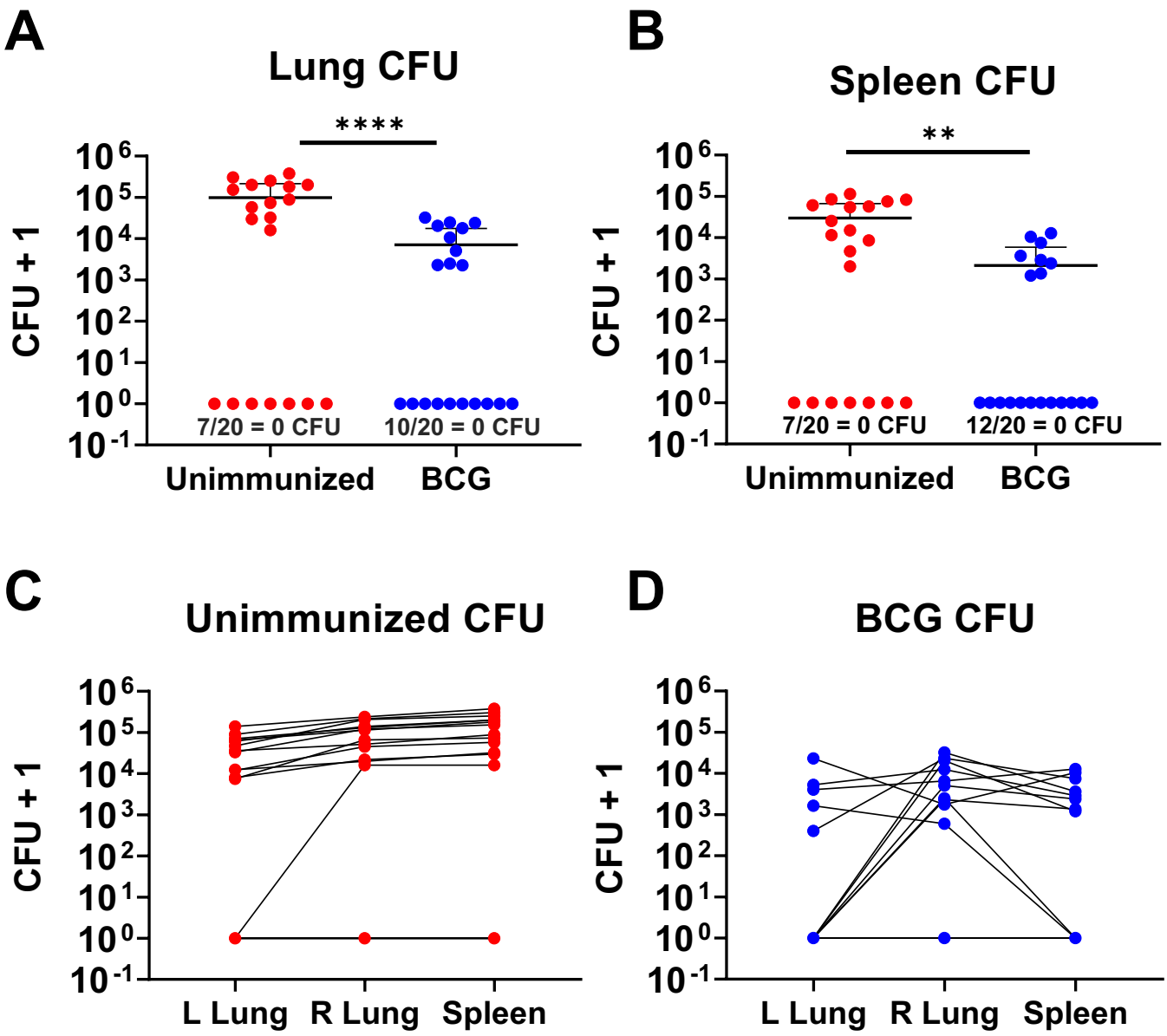
A
Lung CFU
****
CFU + 1
7/20 = 0 CFU
10/20 = 0 CFU
Unimmunized
BCG
B
Spleen CFU
**
CFU + 1
7/20 = 0 CFU
12/20 = 0 CFU
Unimmunized
BCG
C
Unimmunized CFU
CFU + 1
L Lung
R Lung
Spleen
D
BCG CFU
CFU + 1
L Lung
R Lung
Spleen

Figure 2

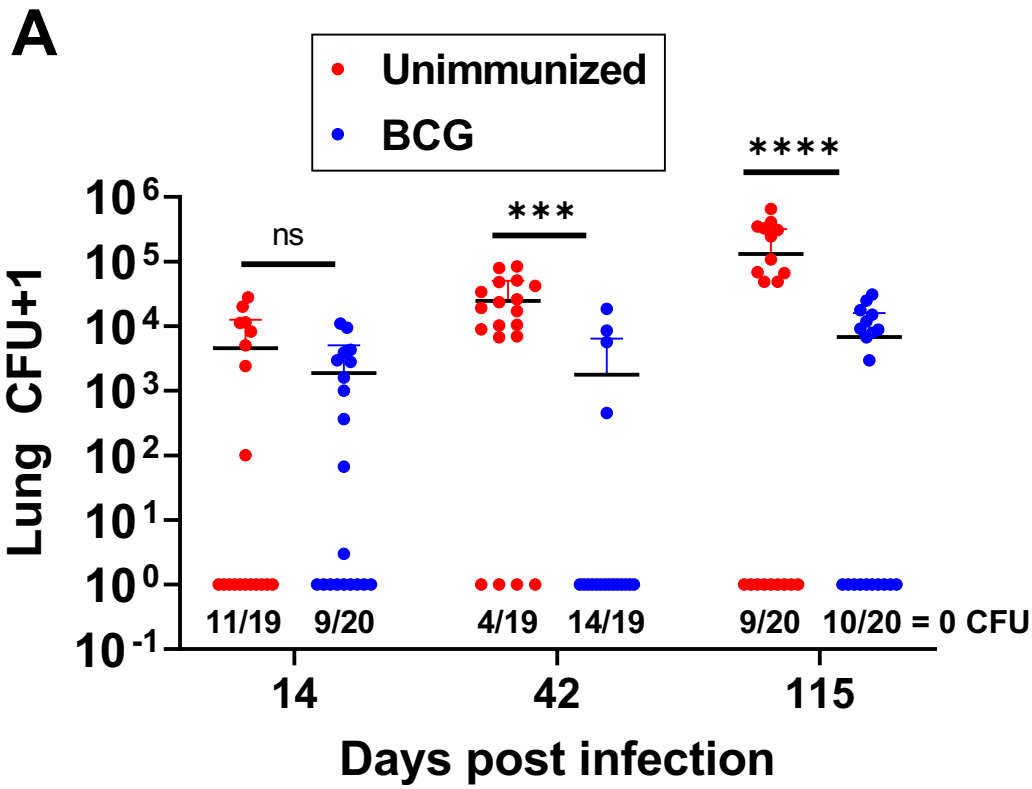
A
Unimmunized
BCG
ns
***
****
Lung CFU+1
10^6
10^5
10^4
10^3
10^2
10^1
10^0
10^{-1}
11/19
9/20
4/19
14/19
9/20
10/20 = 0 CFU
14
42
115
Days post infection

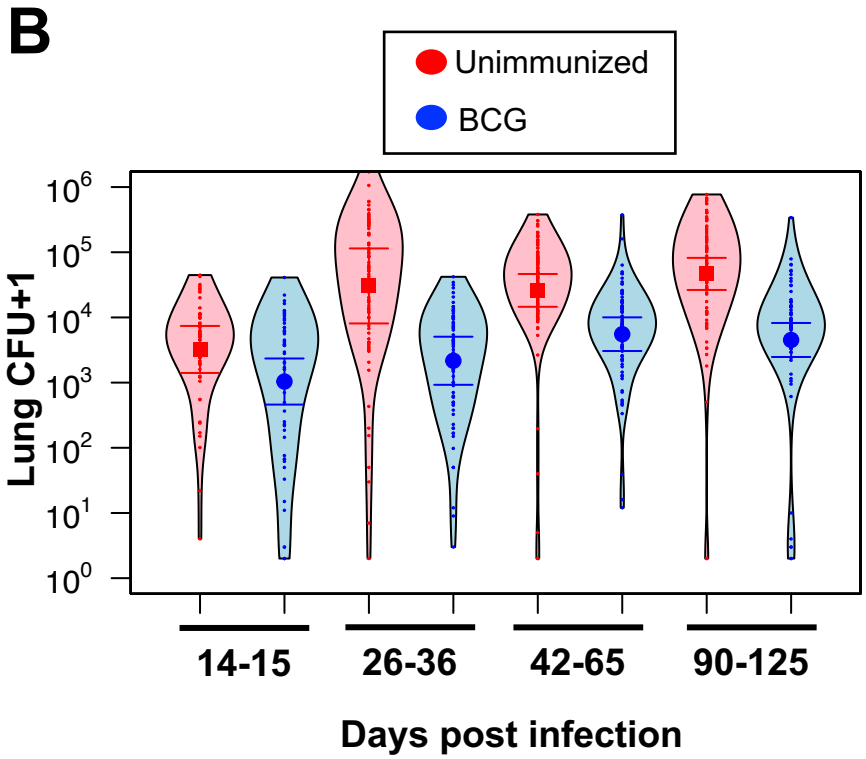
B
Unimmunized
BCG
Lung CFU+1
10^6
10^5
10^4
10^3
10^2
10^1
10^0
14-15
26-36
42-65
90-125
Days post infection

Figure 3

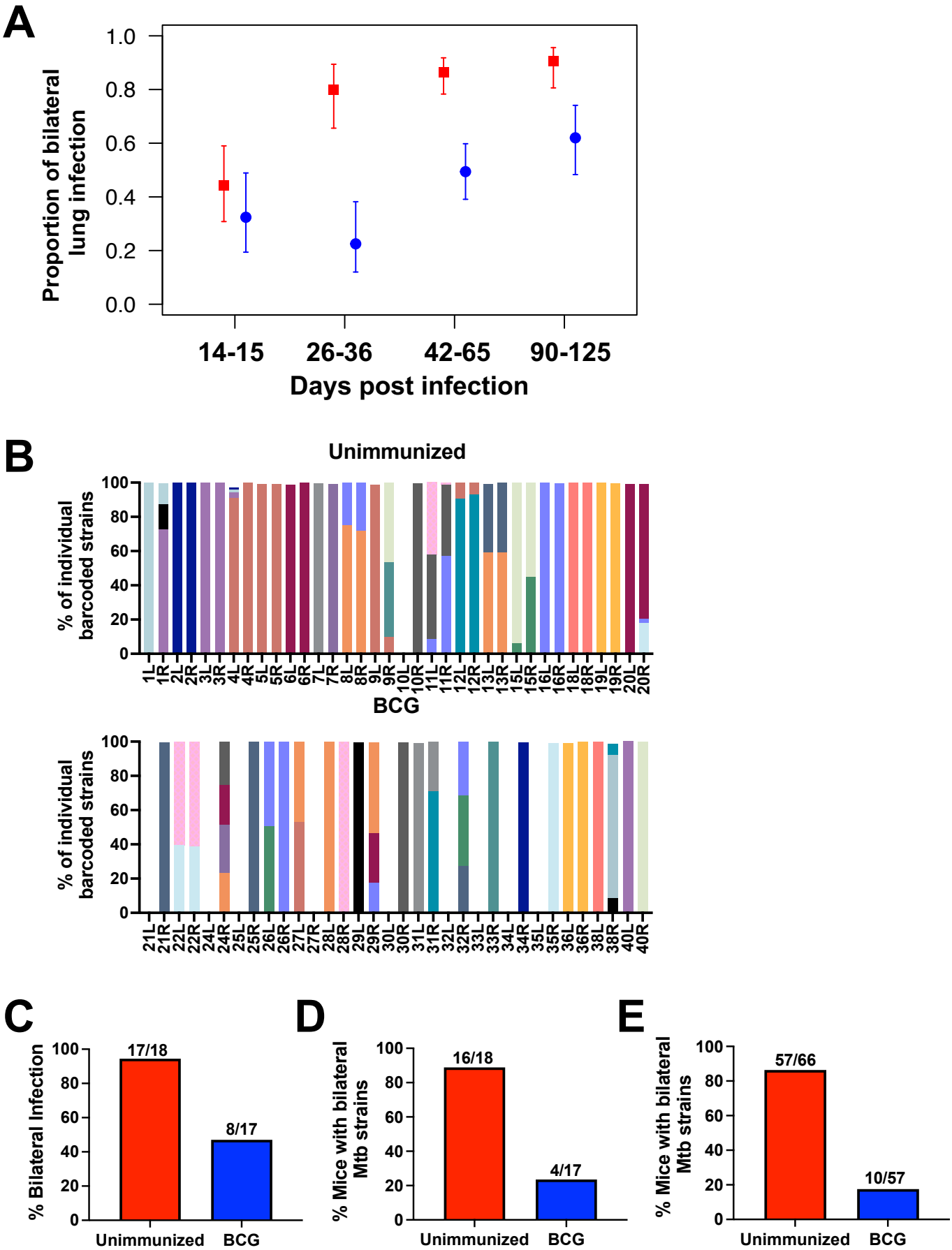
A
Proportion of bilateral lung infection
1.0
0.8
0.6
0.4
0.2
0.0
14-15
26-36
42-65
90-125
Days post infection
B
Unimmunized
% of individual barcoded strains
100
80
60
40
20
0
1L 1R 2L 2R 3L 3R 4L 4R 5L 5R 6L 6R 7L 7R 8L 8R 9L 9R 10L 10R 11L 11R 12L 12R 13L 13R 15L 15R 16L 16R 18L 18R 19L 19R 20L 20R
BCG
% of individual barcoded strains
100
80
60
40
20
0
21L 21R 22L 22R 24L 24R 25L 25R 26L 26R 27L 27R 28L 28R 29L 29R 30L 30R 31L 31R 32L 32R 33L 33R 34L 34R 35L 35R 36L 36R 38L 38R 40L 40R
C
% Bilateral Infection
100
80
60
40
20
0
17/18
8/17
Unimmunized
BCG
D
% Mice with bilateral Mtb strains
100
80
60
40
20
0
16/18
4/17
Unimmunized
BCG
E
% Mice with bilateral Mtb strains
100
80
60
40
20
0
57/66
10/57
Unimmunized
BCG

Figure 4

A

	# mice with undetectable CFU (Unimmunized)	# mice with undetectable CFU (BCG)
All timepoints w/o D14-15	154/440 (35.0%)	191/443 (43.1%)
14-15 dpi	41/97 (42%)	41/100 (41%)
26-36 dpi	34/118 (29%)	40/116 (35%)
42-65 dpi	54/164 (33%)	65/162 (40%)
90-125 dpi	66/158 (42%)	86/165 (52%)

B

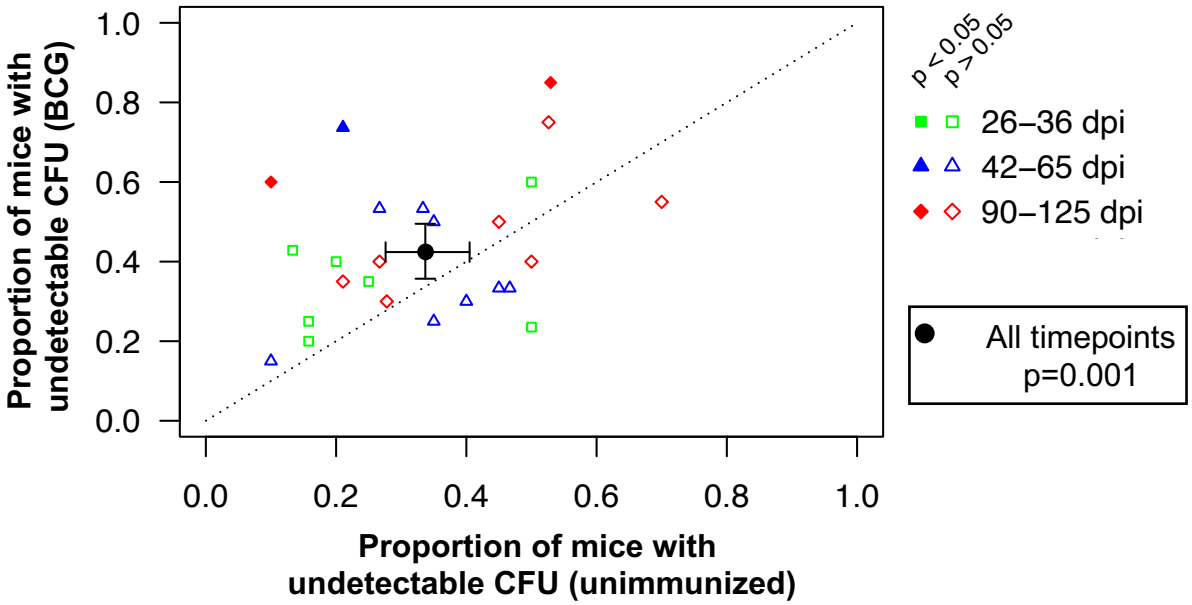

C

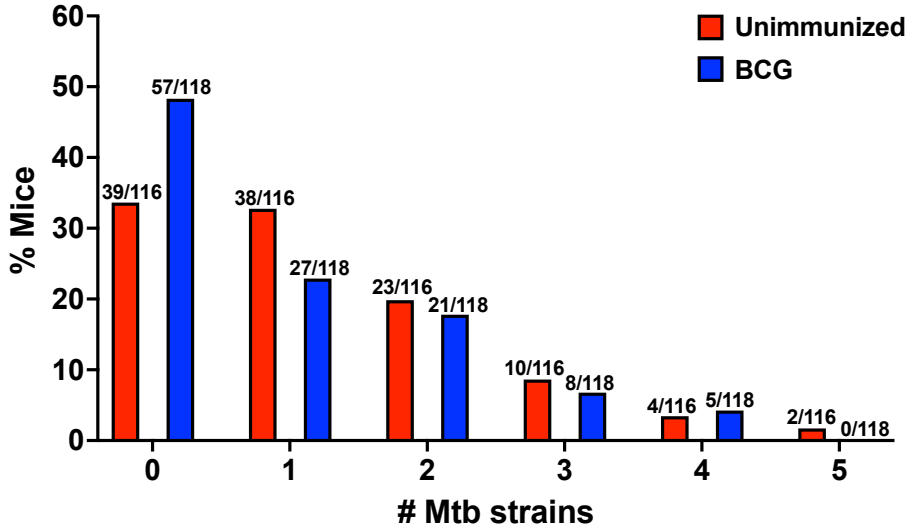

Figure 5

		Min. sample size per group	
Prevalence	**Vaccine efficacy**	**80% Power**	**90% Power**
61.6%	20%	259	342
61.6%	30%	112	155
61.6%	40%	66	84
61.6%	50%	40	55
61.6%	60%	28	37
61.6%	70%	21	25
61.6%	80%	16	18
61.6%	90%	12	16

Table 1